Structural and Energetic Preferences of π, σ, and Bidentate Cation Binding (Li^+, Na^+, and Mg^{2+}) to Aromatic Amines ($Ph-(CH_2)_n-NH_2$, $n = 2-5$): A Theoretical Study

J. Srinivasa Rao and G. Narahari Sastry*

Molecular Modeling Group, Indian Institute of Chemical Technology, Tarnaka, Hyderabad 500 607, India

Received: December 17, 2008; Revised Manuscript Received: February 24, 2009

MP2/aug-cc-pVTZ calculations have been carried out to systematically explore three distinct binding preferences, namely, monodentate binding in π and σ fashions to aromatic and amine groups, respectively, and the bidentate mode of Li^+, Na^+ and Mg^{2+} ions with aromatic amines ($Ph-(CH_2)_n-NH_2$, $n = 2-5$). Several model systems were devised to examine the binding strength of the interactions where the aromatic and amine motifs are not interconnected. The sensitivity of structures and energetics to the basis set superposition error (BSSE) was examined by doing the geometry optimization with a counterpoise option at the MP2/6-31G(d) and MP2/cc-pVDZ levels. Variations in the binding affinities of Li^+, Na^+, and Mg^{2+} metals to π systems and $-NH_2$ groups are observed. The effects of the spacer chain orientation and its length on the binding of metal ions and protons to aromatic amines are studied. It is observed that Mg^{2+} binding is sensitive to the spacer chain orientation and its length, whereas Li^+ or Na^+ binding is independent of spacer chain orientation and length. Reorganization energies are estimated for the complexation of metal ions to aromatic amines. It is observed that the reorganization energy for the complexation of Mg^{2+} is slightly higher than that of Li^+, Na^+, and H^+.

Introduction

Understanding the factors responsible for the adoption of three-dimensional structures of macromolecules in general and folding of proteins in particular has been one of the most fascinating aspects in biology and chemistry. While, in general, the linear and stretched macromolecular conformations are entropically favored, molecules tend to twist and warp, guided by the stabilizing intramolecular noncovalent interactions. The hydrogen bonding and stacking interactions have been recognized as the most important ones and have been extensively studied.[1−6] The roles of cation$-\pi$ interactions, the C$-$H$-\pi$ interaction, and other types of noncovalent interactions in controlling the supramolecular assembly have received much attention in recent years and are the subjects of rigorous experimental and theoretical studies.[7−15] This is an area where the interplay between theory and experiment appears to be highly useful to understand the factors responsible for adopting a given three-dimensional molecular structure.[1] Metal aromatic interactions are ubiquitous in both chemistry and biology and are generally responsible for the structure, function, and regulation of processes of biological interest.[5,6,13,15] The structural changes commensurate with the complexation of metal ions to aromatic amino acid residues are implicated in a range of biochemical and biophysical processes.[16−18] A combined experimental and computational study on the alkali metal ions' complexation with dipeptides showed significant changes for different DFT functionals. This study concluded that, depending on the size of metal ions, the chelating and nonchelating conformations are competitive in their complexation energies.[16] The current authors have examined the contrasting ways in which the proton and metal ion bind to the α,ω-diamines when they bind in a mono- and bidentate fashion, along with the experimental colleagues.[19] Earlier studies reveal that there is a substantial cation$-\pi$ effect in stabilizing the chelating conformations of metal aromatic amino acid complexes.[20−22] Competitive interaction between cation$-\pi$ and cation$-\sigma$ interactions within the same molecules was evaluated using quantum chemical calculations.[21] This study concluded that cation$-\pi$ interactions are competitive with cation$-\sigma$ interactions and play an important role in stabilizing the chelating conformations. Recently, a combined experimental and theoretical study examined the effect of the cation$-\pi$ interaction on the stabilization of organolithium complexes; this study concluded that the amount of stabilization gained by complexation of Li^+ with π systems is quite comparable with that for Li$-$N and Li$-$O interactions.[23]

Thus, the earlier observations reveals the importance of a metal ion containing the three-dimensional structures of macromolecules. The two principle interactions in which metal ions engage in proteins are cation$-\pi$ interactions and σ interactions with amines, besides the coordination of the metal ion with the side chain of acidic residues.

Clearly, the importance of interactions involving aromatic and amine motifs and the frequency of occurrences and participation in the key functions of biological relevance is only next to that for the hydrogen bonding. In the current study, we have considered aromatic amines having the spacer chain length from 2 to 5 carbon atoms as model systems to examine the cation (Li^+, Na^+, and Mg^{2+}) complexation. The relative variations of the binding strengths as a function of the spacer group have been estimated with respect to the reference model system. The current study is aimed to address the following questions, which will be of relevance to understand the effect of the metal ion on the structures of selected molecules of biological interest. What is the relative preference of Li^+, Na^+, and Mg^{2+} to bind with an aromatic ring in a π fashion and of amines to bind in a σ fashion? How do the metal conformations compare with those of protonated ones? How much of the structural reorganization is required to achieve the bidentate conformations? Very

* To whom correspondence should be addressed. E-mail: gnsastry@gmail.com.

10.1021/jp811124g CCC: $40.75
Published on Web 04/09/2009

TABLE 1: Interaction Energies (in kcal/mol) of Different Model Systems Calculated at the MP2/aug-cc-pVTZ//MP2/cc-pVDZ Level

	counterpoise-uncorrected			counterpoise-corrected		
complex	Li^+	Na^+	Mg^{2+}	Li^+	Na^+	Mg^{2+}
M−NH$_3$	−38.4	−26.0	−94.2	−38.6	−26.1	−94.5
M−Tol	−38.9	−23.9	−123.8	−39.6	−24.4	−124.6
M−B	−36.1	−22.0	−115.4	−36.9	−22.6	−116.3
M−B−NH$_3$	−40.4	−27.9	−133.0	−41.1	−28.5	−133.9
M−NH$_2$−Me	−40.5	−27.1	−104.6	−40.7	−27.2	−104.9
NH$_3$−M−B	−68.0	−44.4	−187.1	−69.1	−44.6	−188.4
M−NH$_3$−B	−48.6	−32.6	−121.2	−48.9	−32.8	−121.6

reliable ab initio and density functional methods have been employed to quantitatively estimate the binding energies and also evaluate the structures and explore the structure−binding energy relationships.

Methodology Section

All of the systems considered in the study were subjected to the geometry optimizations at the MP2 level using 6-31G(d) and cc-pVDZ basis sets. Performing geometry optimizations at bigger basis sets was practically prohibited considering the size of the systems under study. In order to estimate the inadequacy of basis sets in computing the interaction energies and geometries of intermolecular complexes, geometry optimizations were performed at the MP2 level with the 6-31G(d) and cc-pVDZ basis sets by including the counterpoise correction. Recently, we have reported a systematic study on the metal ion interaction with water clusters. MP2 appears to be more reliable compared to the popular density functional theory functional B3LYP.[24] Boys and Bernardi's[25] counterpoise calculations were performed with "Counterpoise = N" option for all fragments in the complex. However, single-point energy values could be evaluated at the MP2/aug-cc-pVTZ level on the optimized geometries obtained at the MP2/cc-pVDZ level (using the counterpoise method). The reorganization energy upon the complexation of a metal ion to aromatic amines was estimated by taking the energy difference of the aromatic amine motifs before and after complexation with the metal ion or proton in their respective sites. Thus, if the reorganization energy is higher, it indicates that the aromatic amine motif undergoes a major structural reorganization to optionally bind with the metal ion or proton. Reduced variational space (RVS) energy decomposition analysis was done for some of the model systems considered using the HF/6-31G(d,p) wave function.[26] Natural population analysis (NPA) was used to examine the charge transfer from the N atom and π electrons of aromatic amines to Li^+, Na^+, and Mg^{2+} ions. NPA calculations were done at the HF/cc-pVTZ level of theory. The interaction energies of metal ions with aromatic amines were calculated in the following way.

$$\Delta E_{\text{int}} = E_{\text{Complex}} - (E_{\text{A.A}} + E_{\text{M}})$$
$$\text{Complex} = \text{A.A}\cdots\text{M} \qquad \text{M} = Li^+,\ Na^+,\ Mg^{2+},\ \text{and } H^+$$
$$\text{A.A (Aromatic Amine)} = \text{Ph}-(CH_2)_n-NH_2 \qquad n = 2-5 \tag{1}$$

All calculations were done using Gaussian 03 suite of programs.[27]

Results and Discussions

Interaction Energies. The interaction energy (IE) values of the model systems are compiled in Table 1. Unless otherwise mentioned, all IEs were discussed at the MP2/aug-cc-pVTZ level. As shown in Schemes 1 and 2; the nomenclature is given based on the site of attack, whether the complex is a linear or cyclic one, and the number of carbon atoms in the spacer chain. Throughout the manuscript, the nomenclature cis and trans is used for the complexes (**M−nl−t** and **M−nl−b**) having a spacer chain orientation in the same or opposite direction of the metal ion, respectively.

SCHEME 1

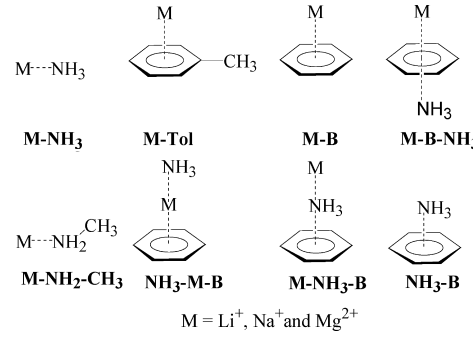

SCHEME 2

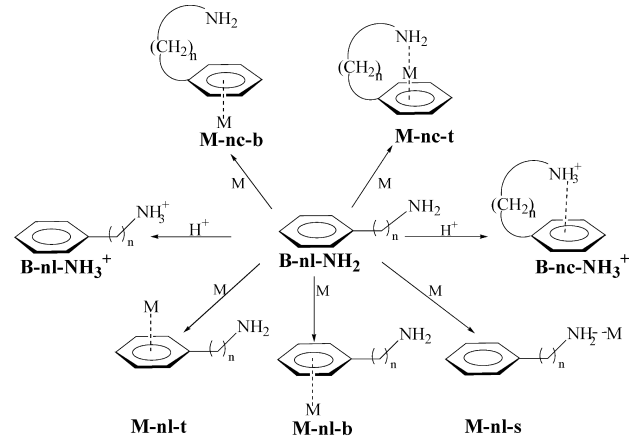

It is observed that the IE of Li^+ with an amine group is about 2.3 kcal/mol higher compared to the Li−π IE of the **Li$^+$−B** complex. Similarly, the IE of Na^+ with an amine group is 4.5 kcal/mol higher than the Na−π IE in the **Na$^+$−B** complex. In contrast, the IE of Mg^{2+} with an amine group is about 22 kcal/mol lower than that of the Mg^{2+}−π IE in **Mg^{2+}−B**. This apparent disparity in the preference of metal ion (Mg^{2+} versus Li^+/Na^+) complexation to the amine and aromatic motifs prompted us to undertake energy decomposition analysis to identify the origin of the differences in various components of total interaction energies. Energy decomposition analysis has been carried out on two simple complexes (**M−NH$_3$** and **M−B**; M = Li^+, Na^+, and Mg^{2+}) to check the various energy components which are responsible for the differences in the

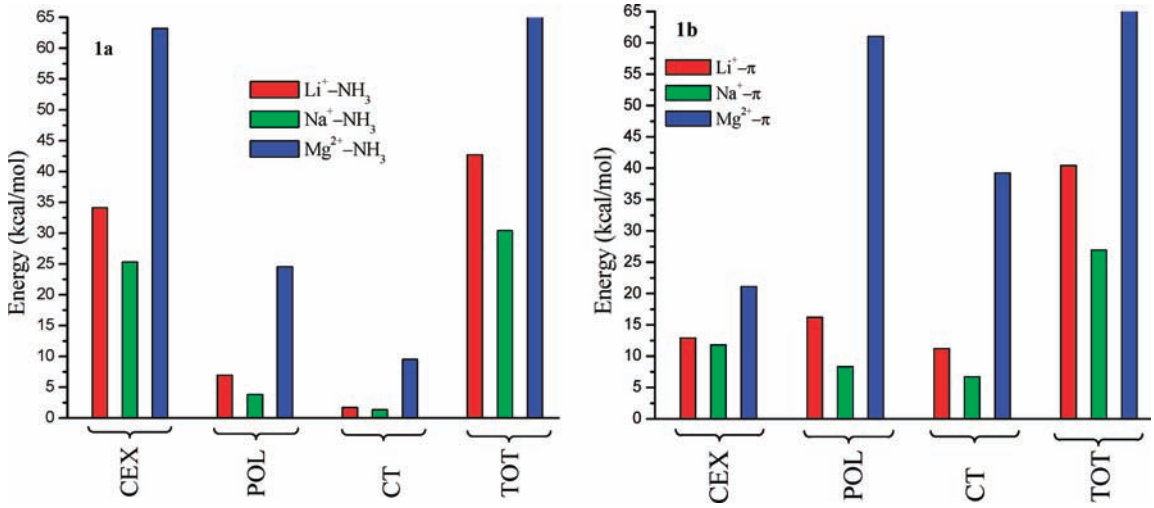

Figure 1. Comparison of different energy terms of **M−NH$_3$** (1a) and **M−B** (1b) (B = benzene; M = Li^+, Na^+, or Mg^{2+}) complexes obtained from RVS analysis. CEX = coulomb exchange energy, POL = polarization energy, CT = charge-transfer energy, and TOT = total interaction energy. All values are in kcal/mol.

TABLE 2: Interaction Energies (in kcal/mol) of Metal−Aromatic Amine Complexes Calculated at the MP2/aug-cc-pVTZ//MP2/cc-pVDZ Level

	counterpoise-uncorrected			counterpoise-corrected		
complex	Li^+	Na^+	Mg^{2+}	Li^+	Na^+	Mg^{2+}
M−2 L−t	−38.0	−23.5	−132.6	−38.7	−24.0	−133.5
M−2 L−b	−38.7	−23.8	−124.3	−39.4	−24.3	−125.2
M−2 L−s	−41.8	−27.6	−129.6	−42.1	−27.8	−130.1
M−2c−t	−59.1	−39.3	−177.2	−59.9	−39.9	−178.3
M−2c−b	−40.4	−24.6	−130.8	−41.1	−25.1	−131.6
M−3 L−t	−38.0	−23.1	−145.9	−38.8	−23.6	−146.9
M−3 L−b	−38.3	−23.1	−124.2	−39.0	−23.6	−125.1
M−3 L−s	−42.1	−28.1	−118.8	−42.3	−28.3	−119.1
M−3c−t	−62.9	−39.3	−186.9	−63.9	−39.9	−188.0
M−3c−b	−40.5	−24.4	−134.6	−41.2	−24.9	−135.5
M−4 L−t	−38.8	−24.0	−133.0	−39.5	−24.5	−133.9
M−4 L−b	−39.5	−24.4	−126.6	−40.2	−24.9	−127.5
M−4 L−s	−43.2	−28.4	−130.2	−43.9	−28.6	−130.7
M−4c−t	−64.6	−40.9	−191.6	−65.6	−41.6	−192.7
M−4c−b	−42.6	−26.8	−136.4	−43.3	−27.3	−137.3
M−5 L−t	−39.0	−24.0	−133.9	−39.7	−24.5	−134.8
M−5 L−b	−38.7	−24.6	−127.3	−39.3	−25.0	−128.2
M−5 L−s	−43.2	−28.9	−130.7	−43.9	−29.1	−131.2
M−5c−t	−59.9	−43.1	−194.8	−60.9	−43.3	−196.0
M−5c−b	−42.3	−26.6	−137.2	−43.0	−27.0	−138.1

interaction energies. Figure 1 shows the contribution of various energy components to the total interaction energy for **M−NH$_3$** (1a) and **M−B** (1b). As we can see from the plots, the energy terms polarization (POL) and charge transfer (CT) are important for M−π, and the coulomb exchange energy (CEX) is important for the **M−NH$_3$** interaction. From the plots of Figure 1a and 1b, it is clear that the POL and CT terms are higher for Mg^{2+} compare to those for Li^+ and Na^+, which produces the differences in the IEs. The higher polarizability of Mg^{2+} is responsible for the preferential binding to the π system. The IE of Li^+ with **NH$_2$−Me** is almost comparable (1 kcal/mol) with the IE of the **Li$^+$−Tol** complex, whereas the IE of Mg^{2+} with toluene is about 20 kcal/mol higher than its IE with **−NH$_2$−Me**. The above two observations show that when π- and σ-donor groups are in the isolated form, Mg^{2+} prefers to bind in a π fashion, while Li^+ and Na^+ prefer to bind in a σ fashion. Comparison of the M−π IE in **M−B** with the M−π IE of the **M−B−NH$_3$** complex gives the following results. The presence of an NH_3 group below the plane of the π system enhances the Li^+ IE by about 4 kcal/mol, the Na^+ IE by 6 kcal/mol, and the Mg^{2+} IE by about 16 kcal/mol. Expectedly, the bidentate complexation (**NH$_3$−M−B**) of metals with the NH_3 and π system produces higher IEs than corresponding monodentate (**M−B** and **M−NH$_3$**) complexes. From Table S1 (Supporting Information), it is clear that the basis set superposition error (BSSE) is more significant in the case of bidentate (5−6 kcal/mol) complexes compared to that for the corresponding monodentate (1−2 kcal/mol) complexes.

The IEs for all metal−aromatic amine complexes at the MP2/aug-cc-pVTZ//MP2/cc-pVDZ level are depicted in Table 2. The IE of Li^+ and Na^+ with an amine group is about 3−5 kcal/mol higher than that of its IE with an aromatic ring in all cases (n = 2−5) studied. As pointed out earlier in Figure 1, POL and CT energies are dominant contributions to the strength of M−π interactions which clearly account for the much higher propensity of the Mg^{2+} ion to have a cation−π interaction compared with its monocationic counterparts, Na^+ and Li^+. The IEs of the complexes **M−nl−t** and **M−nl−b** (M = Li^+ and Na^+) show that the spacer chain orientation does not show a significant effect on the Li^+ and Na^+ complexation with the aromatic ring.

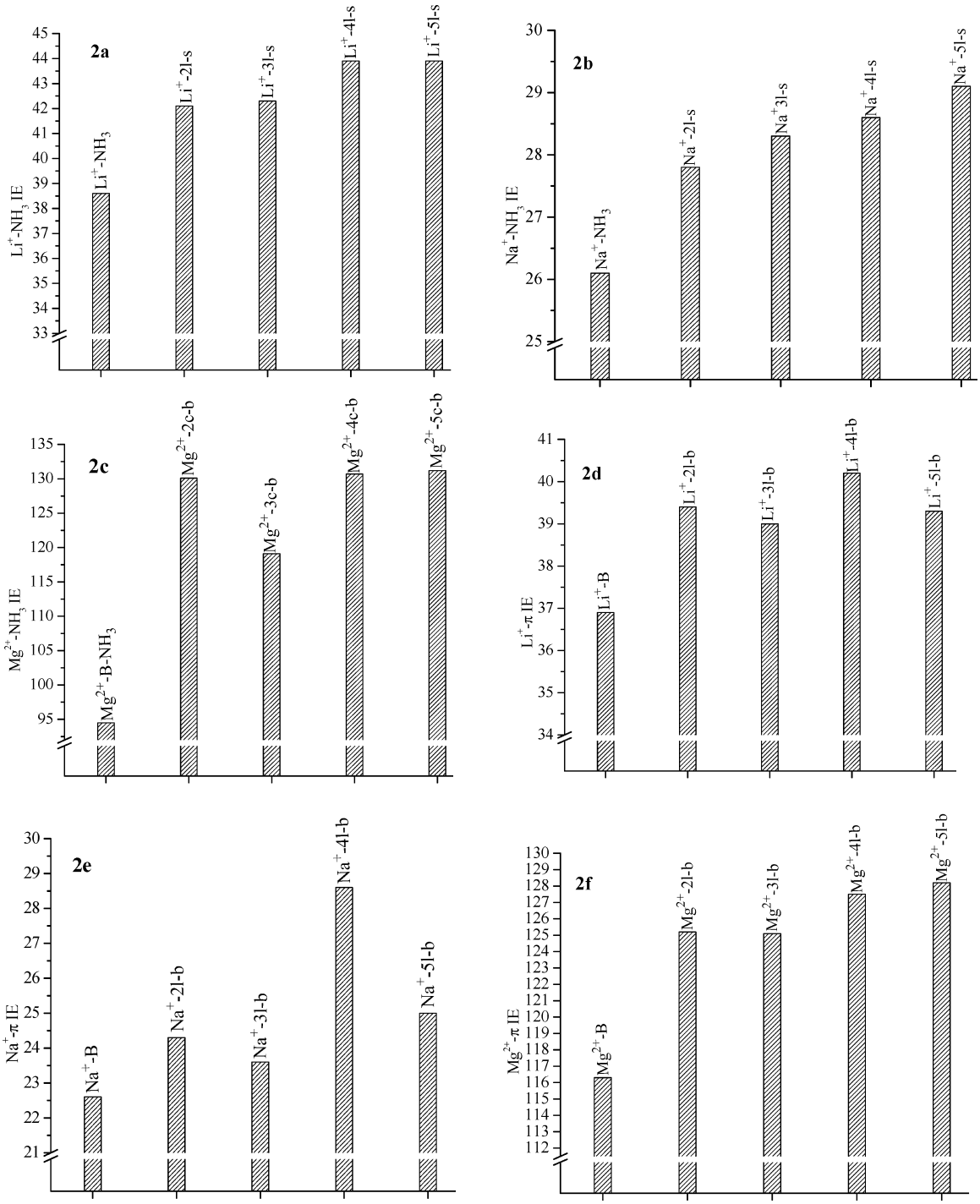

Figure 2. Correlation of interaction energies (IE) (in kcal/mol) of various complexes with the spacer chain length of aromatic amines at the MP2/aug-cc-pVTZ level.

Thus, the IE of Li^+ and Na^+ with either NH_2 or the π system does not vary significantly (within 1.5 kcal/mol) with the spacer chain length. In general, depending on the site of attack, the counterpoise-corrected and -uncorrected IEs of the Li^+ and Na^+ complexes alter between 1 and 1.5 kcal/mol. This shows that at the aug-cc-pVTZ level, basis set superposition errors do not alter the interaction energies appreciably. It is noticed that, irrespective of the spacer chain length, the BSSE values for a bidentate complex at the 6-31G(d) basis set are about 10−11 kcal/mol. However, increasing the size of the basis set (aug-cc-pVTZ) decreases the BSSE value to 1.5 kcal/mol. For monodentate complexes (**M**−**nl**−**s**), the IEs of counterpoise-corrected and -uncorrected values alter between 2 and 5 kcal/mol. These observations show that the bidentate complexes are more sensitive to the quality of the basis set, and the 6-31G(d) basis set is clearly inadequate to model these complexes.

Unlike Li^+ and Na^+ complexation, the Mg^{2+} complexation is sensitive to the spacer chain orientation and its length. From Table 2, for $n = 2$, the Mg−π IE of the cis complex is about 8 kcal/mol higher than that of the corresponding trans complex. For the complex with $n = 3$, the cis form has an IE that is 20 kcal/mol higher than the corresponding trans form; this is due to a through-space interaction of Mg^{2+} with an amine group in the cis complex. For $n = 4$ and 5, the IE of the cis complex is about 3−5 kcal/mol higher than that of the trans complexes. From these observations, one can see that the charge and size

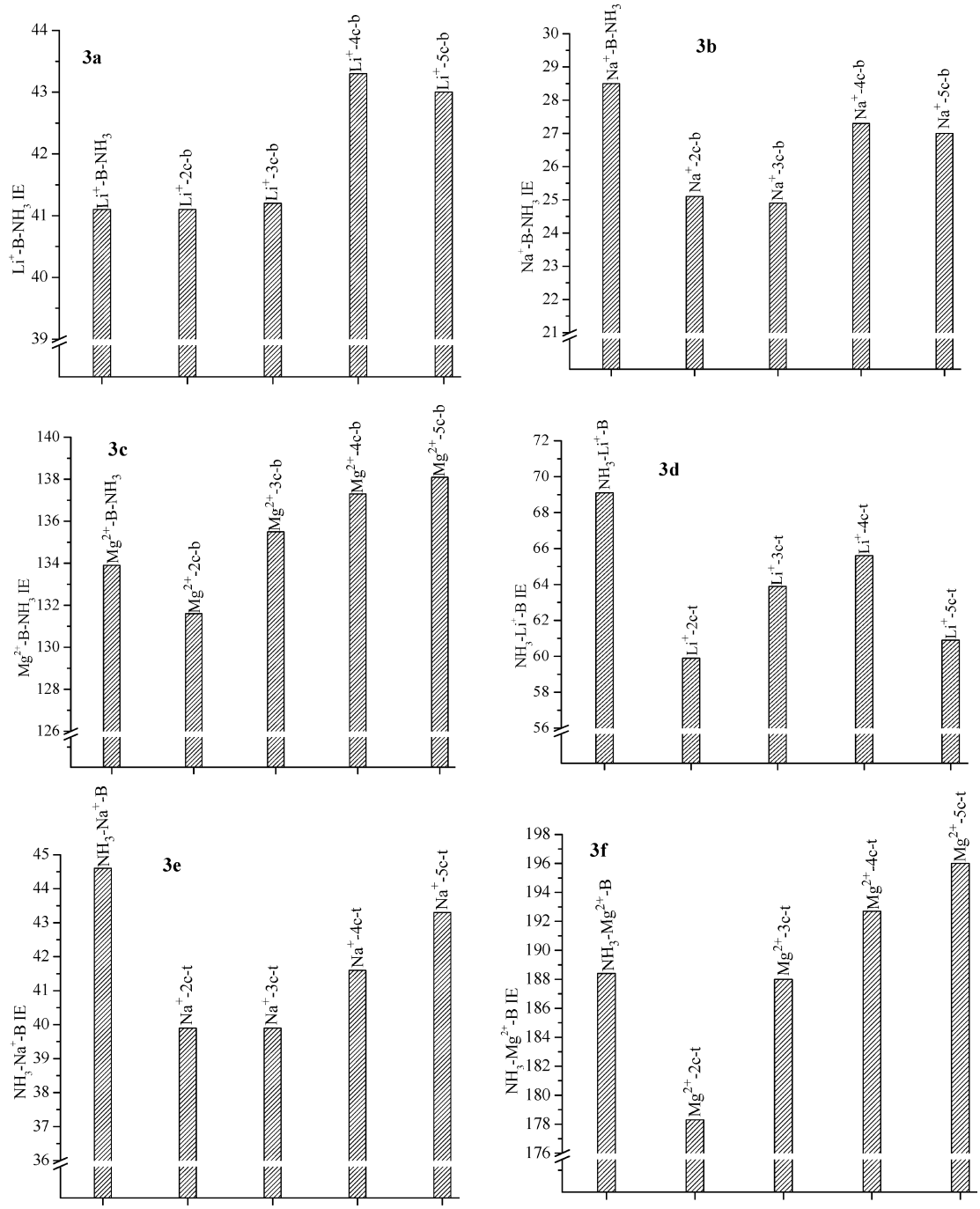

Figure 3. Correlation of interaction energies (IE) (in kcal/mol) of various complexes with the spacer chain length of aromatic amines at the MP2/aug-cc-pVTZ level.

of the metal play important role in these complexes. The bidentate chelation of Mg^{2+} with aromatic amines is sensitive to the spacer chain length. For example, the complex **Mg^{2+}−3c−t** has a 10 kcal/mol higher IE than that of the **Mg^{2+}−2c−t** complex. However, increasing the spacer chain length ($n = 4$ and 5) increases the IE by about 4 kcal/mol. For the complexes **Mg^{2+}−nc−b**, the metal ion binds with an aromatic ring from one plane along the centroid, and the amine group orients along the centroid of the aromatic ring from the opposite plane. The IEs of these types of complexes are slightly higher (2−3 kcal/mol) than the complexes wherein the spacer chain orients in a linear fashion. From mono- to bidentate complexes, the increase in the IEs of Mg^{2+} complexes is three-fold greater than that for Li^+ and Na^+ complexes. Correlation of the IEs of Li^+, Na^+ and Mg^{2+} in their mono- and bidentate forms for various complexes without a spacer chain (model systems) and with different spacer chain lengths was made at the MP2/aug-cc-pVTZ level; the plots are available in Figures 2 and 3. From the plots of Figure 2a and b, it is clear that the IE of the model system (**M−NH$_3$**; M = Li^+ and Na^+) is 2−5 kcal/mol less than the IE of Li^+ or Na^+ with the amine group of aromatic amines. Expectedly, due to the inductive effect caused by methyl groups which are attached to amines, as the chain length increases, the IEs increase gradually. The IE of Mg^{2+} with NH_3 is about 35 kcal/mol less than the interaction of Mg^{2+} with the amine group of the aromatic amine. This may be due to the through-space interaction of Mg^{2+} with an aromatic ring. Except for $n = 3$, all other Mg^{2+} complexes have similar IEs (∼130 kcal/mol) with the amine group (see Figure 2c). Similarly, if we compare the M−π IEs of model systems

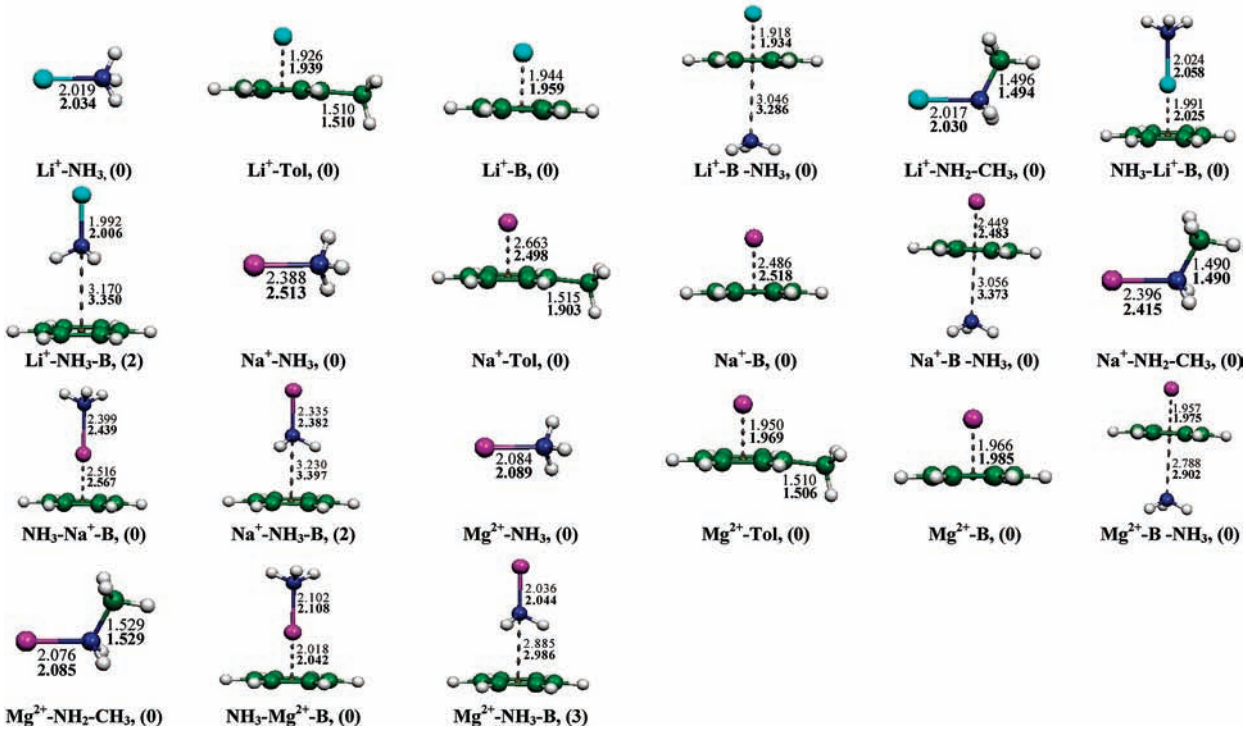

Figure 4. Geometrical parameters of model systems optimized by using the counterpoise method (bold) and without using the counterpoise method (normal) at the MP2/cc-pVDZ level. Bond lengths are in Å. NIMAG values are given in parentheses.

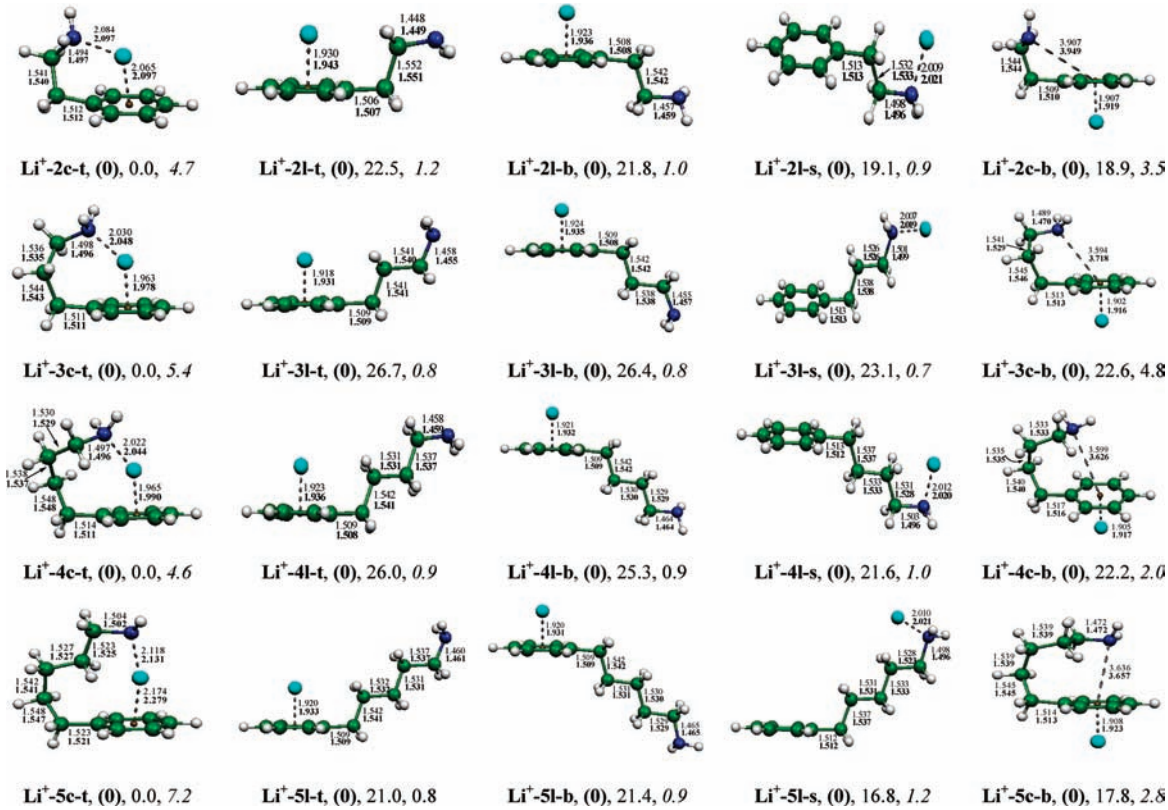

Figure 5. Geometrical parameters of Li^+−aromatic amine complexes optimized by using the counterpoise method (bold) and without using the counterpoise method (normal) at the MP2/cc-pVDZ level. Bond lengths are in Å. NIMAG values are given in parentheses. Relative energies (in kcal/mol) (normal) of all complexes were obtained at the MP2/Aug-cc-pVTZ level. Reorganization energies (in kcal/mol) (italic) of all complexes were obtained at the MP2/aug-cc-pVTZ level.

(**M**−**B**) with the M−π IEs of aromatic amine complexes, clearly, the M−π IE in the aromatic amine complex is higher than the M−π IE of the model systems. However, increasing the spacer chain length of aromatic amines has shown some irregular trends in the interaction energies (see Figure 2d−f). These observations shows that metal−π interactions are enhanced with the introduction of methyl groups as side chains. Figure 3a−c shows the effect of an amine group on metal−π

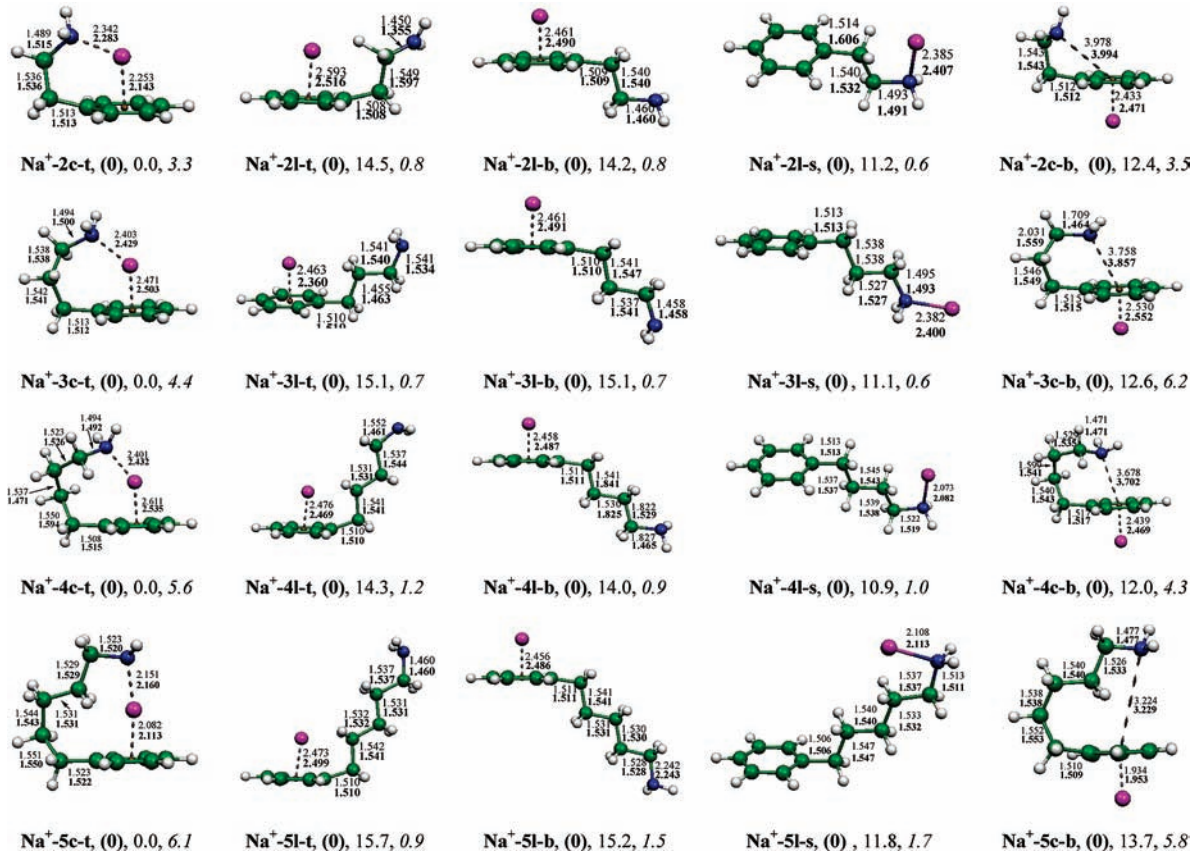

Figure 6. Geometrical parameters of Na^+−aromatic amine complexes optimized by using the counterpoise method (bold) and without using the counterpoise method (normal) at the MP2/cc-pVDZ level. Bond lengths are in Å. NIMAG values are given in parentheses. Reorganization energies (in kcal/mol) (italic) of all complexes were obtained at the MP2/aug-cc-pVTZ level.

interactions; for these complexes, the amine group is present near the π system. As we can see from the plots, Li^+ and Mg^{2+} have higher IEs in aromatic amine complexes than isolated model systems, whereas the Na−π interaction energy is 1−3 kcal/mol higher in the isolated complex than the Na−π interaction energy in aromatic amine complex. From Figure 3d−f, it is observed that for Li^+ and Na^+, bidentate complexation is highly preferred without the side chain (isolated form). However, Mg^{2+} prefers the bidentate chelation for the side-chain length of 3 and above. It is important to note that, in the absence of side chain, the Mg^{2+} complexation energy is relatively higher (9 kcal/mol) compared to that for complexes with side lengths of $n = 2$ and 3; when the side-chain length increases ($n = 4$ and 5), the strain in the backbone of the aromatic amine reduces, and the Mg^{2+} prefers to bind with the aromatic amine.

The proton affinities of the aromatic amines were estimated for both cyclic and linear complexes at the MP2 method with different basis sets, and these are provided in the Supporting Information (Table S6). The relative energies of the protonated cyclic and linear complexes are given in Figure S1 (Supporting Information). Unlike neutral conformations, protonated cyclic and linear conformations have about 5−12 kcal/mol differences in their relative energies. In cyclic complexes, the $-NH_3^+$ interacts with π electrons of the aromatic ring, and this interaction makes the cyclic complex more stable than the linear counterpart. Similarly, the proton affinities of cyclic complexes are about 10 kcal/mol higher than those of linear complexes. As the spacer chain length increases, the proton affinity of the cyclic complex increase from 3 to 11 kcal/mol, while the proton affinity values of linear conformers do not change much with spacer chain length. The reorganization energy upon the complexation of metal ions to aromatic amines at various binding modes was estimated at the MP2/aug-cc-pVTZ level and is given in Figures 5, 6, and 7 and Figure S1 (Supporting Information) for Li^+, Na^+, Mg^{2+}, and H^+, respectively. The reorganization energies are higher for Mg^{2+} than those of Li^+, Na^+, and H^+. Expectedly, reorganization energies are higher for bidentate complexes than the monodentate complexes. Due to through-space interaction of Mg^{2+} with the amine group, the reorganization energies of **Mg^{2+}−2L−t** and **Mg^{2+}−3L−t** are much higher than those of the other linear complexes. As we can see from the Figure 7, these complexes having Mg^{2+} and NH_2 are spatially closer to each other; because of this, the reorganization energy seems to be higher than other similar complexes.

Geometries. The geometrical parameters obtained at the MP2/cc-pVDZ level for model systems are given in Figure 4. Comparison of the metal−nitrogen distance in the **M−NH_3** complex with the metal−π distance in the **M−B** complex shows that Li^+, Na^+, and Mg^{2+} are relatively closer to the π system than the nitrogen of NH_3 group. The presence of a CH_3 group either on the N of the NH_3 group or the C of the benzene ring shortens the M−N or M−π distance. For the complex **NH_3−M−B**, the metal ion binds with both the NH_3 group and the π system simultaneously. The M−N and M−π distances in this complex are slightly longer than that in individual complexes **M−NH_3** and **M−B**. In the case of the **M−NH_3−B** complex, the M−N distance is slightly shorter than that of the M−N distance in the **M−NH_3** complex alone. However, this (**M−NH_3−B**) complex is a higher-order saddle point (for Li^+, Na^+, and Mg^{2+}) on the potential energy surface. The other possibility that we have explored in model systems is the

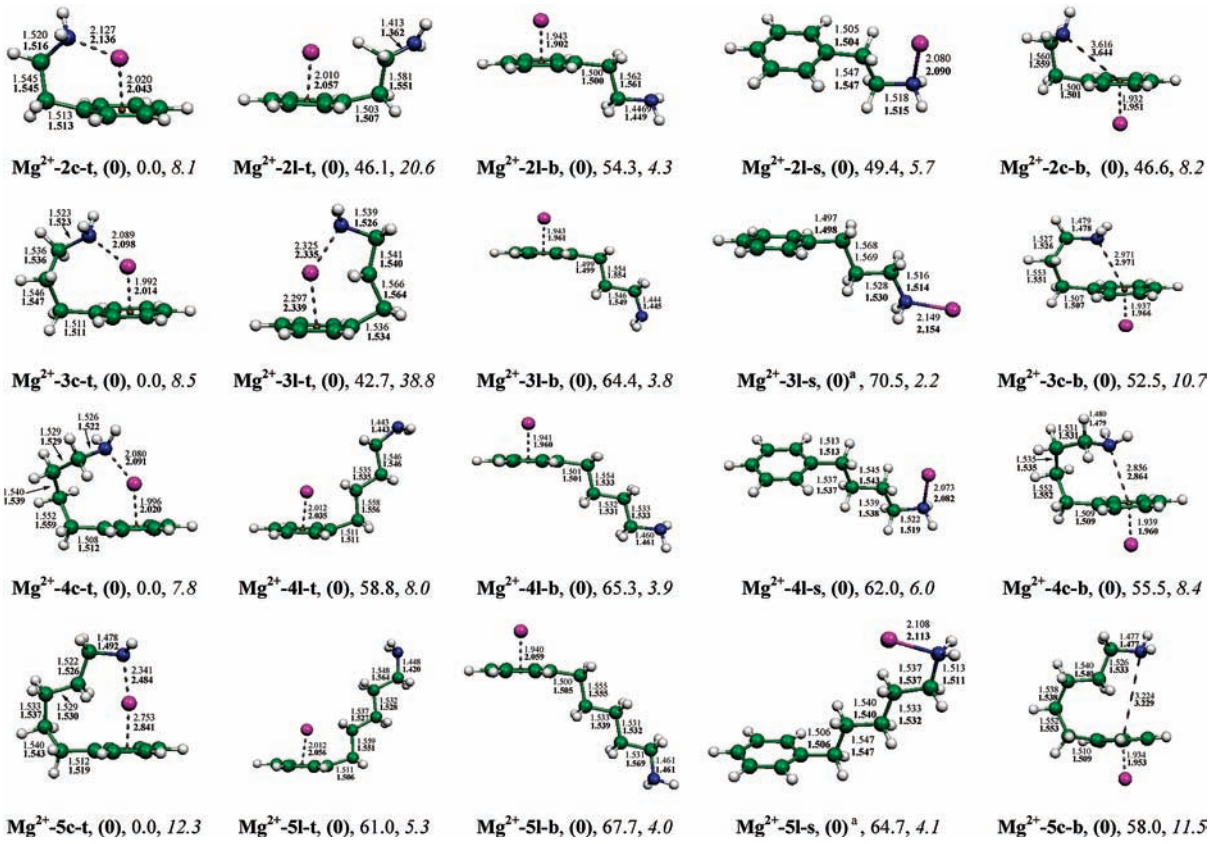

Figure 7. Geometrical parameters of Mg^{2+}−aromatic amine complexes optimized by using the counterpoise method (bold) and without using the counterpoise method (normal) at the MP2/cc-pVDZ level. Bond lengths are in Å. NIMAG values are given in parentheses. [a]Geometrical parameters obtained from the B3LYP/cc-pVDZ level. Relative energies (in kcal/mol) (normal) of all complexes were obtained at the MP2/Aug-cc-pVTZ level. Reorganization energies (in kcal/mol) (italic) of all complexes were obtained at the MP2/aug-cc-pVTZ level.

complexation of the metal ion with the π−NH_3 systems (see **M−π−NH₃** in Figure 4). In this complex, for Li^+, Na^+, and Mg^{2+}, the M−π distance is slightly shorter than that of the M−π distance in bare cation−π systems (without the NH_3 group). Geometry optimizations performed using the counterpoise method gave bond lengths slightly longer than normal (without using the counterpoise option) geometry optimizations.

Figure 5 shows the geometrical parameters obtained for all Li−aromatic amine complexes at the MP2/cc-pVDZ level. All possible binding modes of aromatic amines are explored in the following way; first, the metal ion binds to both the amine and aromatic groups simultaneously (**M−nc−t**), in the second case, the metal ion binds with an aromatic ring in cis and trans positions (**M−nl−t** and **M−nl−b**), in the third case, the metal ion binds with the side-chain amine group (**M−nl−s**), and finally, the metal ion binds from the bottom of the aromatic ring when the spacer chain orients above the plane of the aromatic ring (**M−nc−b**). For the bidentate chelation of the Li^+ ion with aromatic amines, no regular trends were observed in the cation−π distances. The complexes **Li^+−2c−t** and **Li^+−5c−t** have the metal ion symmetrically bound with both the amine group and aromatic ring, and the other complexes have the metal ion a little closer to the aromatic ring (**Li^+−3c−t and Li^+−4c−t**). The cation−π distance in **Li^+−nl−t** (the cis conformation) is slightly shorter than that of the cation−π distance in **Li^+−nl−b** (trans-type conformation). In the case of **Li^+−nl−s** complexes, the Li^+−N distances does not change with the spacer chain length. Relative energies of various complexes are provided in Figures 5, 6, and 7 under each complex. Expectedly, the cyclic bidentate complex has lowest energy on the potential energy surface. It is observed that the relative energies of the cis and trans complexes of Li^+ and Na^+ are within 1 kcal/mol. Similar results are observed for Na^+ complexation with the aromatic amines, and the geometrical parameters are depicted in Figure 6.

Figure 7 shows the geometrical parameters of Mg^{2+}−aromatic amine complexes obtained at the MP2/cc-pVDZ level. In the case of Mg^{2+} complexation, for $n = 3$ and 5, the complexes **M−nl−s** could not be located on the potential energy surface at the MP2 level. However, similar complexes obtained at the B3LYP/cc-pVDZ level were taken and subjected to single-point calculations at the MP2 level. The Mg^{2+}−π distance in cis and trans complexes are influenced by the spacer chain orientation; in cis complexes, the Mg^{2+}−π distance is slightly longer than the Mg^{2+}−π distance of the trans complexes. However, these differences nullify with the increase of spacer chain length. In the case of the complex **Mg^{2+}−2c−t**, the Mg^{2+}−π distance (2.043 Å) is slightly shorter than the Mg^{2+}−N distance (2.136 Å). As the spacer chain length increases, Mg^{2+} binds symmetrically with the $-NH_2$ and aromatic ring. Among all Mg^{2+} complexes, the shortest cation−π distance is seen in **Mg^{2+}−nc−b** complexes. The relative energies of various Mg^{2+}−aromatic amine complexes are provided in Figure 7. The bidentate complexes of Mg^{2+} are about 45−70 kcal/mol more stable than the corresponding monodentate complexes. However, the bidentate complex of Li^+ is about 16−27 kcal/mol more stable than the corresponding monodentate complexes. The geometrical parameters of linear and cyclic conformations of neutral and protonated aromatic amines at the MP2/cc-pVDZ level and the relative energies of cyclic and linear complexes obtained at the MP2/aug-cc-pVTZ level are provided in Figure S1 (Supporting Information). As we can see from the figure,

the differences in the linear and cyclic conformations of neutral aromatic amines are within 1 kcal/mol (except for **B−5n−NH$_2$**), while for the conformation **B−5n−NH$_2$**, the linear complex is about 0.1 kcal/mol more stable than its cyclic form. Protonated cyclic complexes are about 5−12 kcal/mol more stable than their corresponding linear complexes. As the spacer chain length increases, the relative energy increases about 2 kcal/mol. In the case of the protonated cyclic complex, the cationic nature of amine group shortens the distance between the centroid of the aromatic ring and the N of the amine group. Atomic charges were obtained using natural population analysis (NPA) at the HF/cc-PVTZ level and are listed in Tables S7 and S8 (Supporting Information). Expectedly, metal ions are more neutralized in the bidentate form than in the monodentate form. As the spacer chain length increases, the charge transfer from the π cloud of the aromatic ring and the nitrogen of the amine group to the metal ions also slightly increases. Earlier reports from our group revealed that the strength of the caion−π interaction also certainly depends on the size of the π-acceptor systems.[13b,28] Therefore, the aromatic amines with higher chain length are expected to display higher IEs.

Conclusions

The current study illustrates how the metal ion can alter the structural preferences of aromatic amines. Li^+ and Na^+ have displayed a consistently higher propensity to bind with the amine group compared to the aromatic group. In contrast, Mg^{2+} binds more strongly to the π systems compared to the amine group. From the mono- to bidentate, the chelation gain in the binding energy for Mg^{2+} is about three to four times greater than that of Li^+ and Na^+. Thus, cation−π interactions show a higher dependence on the charge of the metal ion compared to that of the cation interaction with lone-pair-bearing molecules. The monodentate binding of metal ions with $-NH_2$ has a small variation in the interaction energies as the spacer chain length increases. Binding of Mg^{2+} to an aromatic ring is sensitive to its side-chain orientation and its length. The Li^+ and Na^+ complexation is independent of spacer chain length and orientation. Structural reorganization due to Mg^{2+} complexation is slightly higher than that due to Li^+ or Na^+ complexation. Thus, the divalent metal ion comlexation leads to a significant variation in the macromolecular structure and the function. The charge on the metal ion depends on the side-chain length and the mode of complexation of metal ions with the aromatic amine (mono- or bidentate).

Acknowledgment. J.S.R. thank CSIR for a senior research fellowship. Ms. K. Jyothsna and Ms. M. Deepthi are thanked for their assistance in doing preliminary calculations. G.N.S. thanks DST for the financial support in the form of Swarnajayanthi fellowship.

Supporting Information Available: Geometrical parameters of neutral and protonated aromatic amines at the MP2/cc-pVDZ level, interaction energies of various complexes obtained at the MP2 level with different basis sets, and NPA charges obtained at the HF/cc-pVTZ level. This material is available free of charge via the Internet at http://pubs.acs.org.

References and Notes

(1) (a) Meyer, E. A.; Castellano, R. K.; Diederich, F. *Angew. Chem., Int. Ed* **2003**, *42*, 1210. (b) Munoz, J.; Sponer, J.; Hobza, P.; Orozco, M.; Luque, F. J. *J. Phys. Chem. B* **2001**, *105*, 6051. (c) Gu, J.; Leszczynski, J. *J. Phys. Chem. A* **2001**, *105*, 10366.

(2) (a) Reddy, A. S.; Vijay, D.; Sastry, G. M.; Sastry, G. N. *J. Phys. Chem. B* **2006**, *110*, 2479. (b) Vijay, D.; Zipse, H.; Sastry, G. N. *J. Phys. Chem. B* **2008**, *112*, 8863.

(3) (a) Suelter, C. *Science* **1970**, *168*, 789. (b) McRee, D. E. *Nat. Struct. Biol.* **1998**, *5*, 8.

(4) (a) Agranoff, D. D.; Krishna, S. *Mol. Microbiol.* **1998**, *28*, 403. (b) Pyle, A. M. *J. Biol. Inorg. Chem.* **2002**, *7*, 679–690. (c) Masson, E.; Schlosser, M. *Org. Lett.* **2005**, *7*, 1923.

(5) (a) Dougherty, D. A.; Stauffer, D. A. *Science* **1990**, *250*, 1558. (b) Kumpf, R. A.; Dougherty, D. A. *Science* **1998**, *261*, 1708–1710. (c) Ma, J. C.; Dougherty, D. A. *Chem. Rev.* **1997**, *97*, 1303.

(6) Chaturvedi, U. C.; Shrivastava, R. *FEMS Immunol. Med. Microbiol.* **2005**, *43*, 105.

(7) Zhu, W.; Luo, X.; Puah, C. M.; Tan, X.; Shen, J.; Gu, J.; Chen, K.; Jiang, H. *J. Phys. Chem. A* **2004**, *108*, 4008.

(8) (a) Tsuzuki, S.; Uchimaru, T.; Mikami, M. *J. Phys. Chem. A* **2003**, *107*, 10414. (b) Quinonero, D.; Garau, C.; Frontera, A.; Ballester, P.; Costa, A.; Deya, P. M. *J. Phys. Chem. A* **2005**, *109*, 4632.

(9) (a) Reddy, A. S.; Sastry, G. N. *J. Phys. Chem. A* **2005**, *109*, 8893. (b) Reddy, A. S.; Zipse, H.; Sastry, G. N. *J. Phys. Chem. B* **2007**, *111*, 11546.

(10) (a) Wall, S. L. D.; Meadows, E. S.; Barbour, L. J.; Gokel, G. W. *Proc. Natl. Acad. Sci. U.S.A.* **2000**, *97*, 6271. (b) Hu, J.; Barbour, L. J.; Gokel, G. W. *Proc. Natl. Acad. Sci. U.S.A.* **2002**, *99*, 512.

(11) (a) Biot, C.; Wintjens, R.; Rooman, M. *J. Am. Chem. Soc.* **2004**, *126*, 6220. (b) McFail-Isom, L.; Shui, X.; Williams, L. D. *Biochemistry* **1998**, *37*, 17105. (c) DeVos, A. M.; Ultsch, M.; Kosssiakoff, A. A. *Science* **1992**, *255*, 306.

(12) Kim, K. S.; Tarakeshwar, P.; Lee, J. Y. *Chem. Rev.* **2000**, *100*, 4145.

(13) (a) Vijay, D.; Sastry, G. N. *J. Phys. Chem. A* **2006**, *110*, 10148. (b) Vijay, D.; Sastry, G. N. *Phys. Chem. Chem. Phys.* **2008**, *10*, 582.

(14) (a) Wouters, J. *Protein Sci.* **1998**, *7*, 2472. (b) Wu, R.; McMahon, T. B. *J. Am. Chem. Soc.* **2008**, *130*, 12554.

(15) Reddy, A. S.; Sastry, G. N. *Proteins: Struct., Funct., Bioinf.* **2007**, *67*, 1179.

(16) Polfer, N. C.; Oomens, J.; Dunbar, R. C. *ChemPhysChem* **2008**, *9*, 579.

(17) Dunbar, R. C.; Polfer, N. C.; Oomens, J. *J. Am. Chem. Soc.* **2007**, *129*, 14562.

(18) (a) Eller, K. In *Organometallic Ion Chemistry*; Freiser, B. S. Ed.; Kluwer: Amsterdam, The Netherlands, 1996; p 123. (b) *Metal Ions in Biology and Medicine*; Etienne, J. C., Khassanovc, Z., Maymard, I., Collery P., Khassanova, L., Eds.; Eurotext: Paris, 2002; Vol. 7, and previous volumes.

(19) Kumar, M. K.; Rao, J. S.; Prabhakar, S.; Vairamani, M.; Sastry, G. N. *Chem. Commun.* **2005**, 1420.

(20) Ryzhov, V.; Dunbar, R. C.; Cerda, B.; Wesdemiotis, C. *J. Am. Soc. Mass Spectrom.* **2000**, *11*, 1036.

(21) Siu, F. M.; Ma, N. L.; Tsang, C. W. *Chem.—Eur. J.* **2004**, *10*, 1966.

(22) Ruan, C.; Rodgers, M. T. *J. Am. Chem. Soc.* **2004**, *126*, 14600.

(23) Monje, P.; Paleo, M. R.; Garcia-Rio, L.; Sardina, F. J. *J. Org. Chem.* **2008**, *73*, 7394.

(24) Rao, J. S.; Dinadayalane, T. C.; Leszczynski, J.; Sastry, G. N. *J. Phys. Chem. A* **2008**, *112*, 12944.

(25) Boys, S. F.; Bernardi, R. *Mol. Phys.* **1979**, *19*, 553.

(26) Stevens, W. J.; Fink, W. H. *Chem. Phys. Lett.* **1987**, *139*, 15. (b) Chen, W.; Gordon, M. S.; *J. Phys. Chem.* **1996**, *100*, 14316.

(27) Frisch, M. J.; Trucks, G. W.; Schlegel, H. B.; Scuseria, G. E.; Robb, M. A.; Cheeseman, J. R.; Montgomery, J. A., Jr.; Vreven, T.; Kudin, K. N.; Burant, J. C.; Millam, J. M.; Iyengar, S. S.; Tomasi, J.; Barone, V.; Mennucci, B.; Cossi, M.; Scalmani, G.; Rega, N.; Petersson, G. A.; Nakatsuji, H.; Hada, M.; Ehara, M.; Toyota, K.; Fukuda, R.; Hasegawa, J.; Ishida, M.; Nakajima, T.; Honda, Y.; Kitao, O.; Nakai, H.; Klene, M.; Li, X.; Knox, J. E.; Hratchian, H. P.; Cross, J. B.; Adamo, C.; Jaramillo, J.; Gomperts, R.; Stratmann, R. E.; Yazyev, O.; Austin, A. J.; Cammi, R.; Pomelli, C.; Ochterski, J. W.; Ayala, P. Y.; Morokuma, K.; Voth, G. A.; Salvador, P.; Dannenberg, J. J.; Zakrzewski, V. G.; Dapprich, S.; Daniels, A. D.; Strain, M. C.; Farkas, O.; Malick, D. K.; Rabuck, A. D.; Raghavachari, K.; Foresman, J. B.; Ortiz, J. V.; Cui, Q.; Baboul, A. G.; Clifford, S.; Cioslowski, J.; Stefanov, B. B.; Liu, G.; Liashenko, A.; Piskorz, P.; Komaromi, I.; Martin, R. L.; Fox, D. J.; Keith, T.; Al-Laham, M. A.; Peng, C. Y.; Nanayakkara, A.; Challacombe, M.; Gill, P. M. W.; Johnson, B.; Chen, W.; Wong, M. W.; Gonzalez, C.; Pople, J. A. *Gaussian 03, Revision C.1*; Gaussian, Inc.: Pittsburgh, PA, 2003.

(28) (a) Priyakumar, U. D.; Sastry, G. N. *Tetrahedron Lett.* **2003**, *44*, 6043. (b) Priyakumar, U. D.; Punnagai, M.; Krishnamohan, G. P.; Sastry, G. N. *Tetrahedron,* **2004**, *60*, 3037.

JP811124G